Radiative Transfer in Thermal Insulations of Hollow and Coated Fibers

K.Y. Wang,* Sunil Kumar,† and C.L. Tien‡
University of California, Berkeley, California

This paper presents a numerical study of radiative transfer in thermal insulation made of hollow cylindrical fibers and of solid fibers coated with thin dielectric films. The radiative properties of the packed fibrous insulation are evaluated from the single-fiber absorption and scattering characteristics that are based on electromagnetic theory. The results show that, for cases of practical interest, hollow fibers have higher backscattered radiation and higher extinction efficiency than solid fibers of the same outside diameter. Thus, insulations made of such are not only of low weight and low heat capacity, but are also more effective in preventing radiative heat loss. Coating solid fibers with thin dielectric films does not appreciably enhance the radiative extinction characteristics, unless the coating is thick or has a high index of refraction.

Nomenclature

a_n, b_n = coefficients in expressions of radiative properties, Eqs. (1-3)
b = backscattered fraction of radiation, Eq. (6)
c = interparticle clearance
D = outside diameter of the fiber
f_v = solid volume fraction, Eq. (8)
$\hat{f}_v$ = apparent volume fraction, Eq. (8)
G = function used in computing backscatter, Eq. (6)
I = intensity
k_r = radiant conductivity
l = mean length of fibers
$\tilde{m}$ = refractive index, $n-ik$
n = real part of the refractive index
N = number of fibers
$Q_{a,e,s}$ = absorption, extinction, and scattering efficiencies, respectively, $Q_e = Q_a + Q_s$
r = radius
T_m = mean temperature
V = volume of the insulation
α = size parameter, Eq. (4)
η = angle of incident relative to fiber orientation, Fig. 1
κ = imaginary (absorptive) part of refractive index
λ = wavelength
ζ = scattering (observation) angle, Fig. 1
σ = Stefan-Boltzmann constant
$\sigma_{a,e,s}$ = absorption, extinction, and scattering coefficients, respectively, $\sigma_e = \sigma_a + \sigma_s$
ω = single-scattering albedo, $= Q_s/Q_e$

Superscript

(-) = averaged over incident angles

Subscripts

0 = surrounding medium
1,2 = outer and inner cylinders, respectively

Received July 7, 1986; revision received Jan. 5, 1987.

*Research Assistant, Department of Mechanical Engineering (presently, Research Engineer, Solar Energy Research Institute, Golden, CO).
†Research Assistant, Department of Mechanical Engineering.
‡A. Martin Berlin Professor, Department of Mechanical Engineering. Fellow AIAA.

Introduction

THE increased utilization of packed fibers and spheres as insulation materials has stimulated many studies on the various heat-transfer mechanisms through these media, such as gas conduction and radiation, and natural convection.[1,2] The recognition of radiation as a dominant heat-transfer mode prompted many detailed studies of radiative transfer, especially through packed fibers,[3,4] packed spheres,[5] and packed opacified fibers and spheres.[6] Analytical models for the thermal radiation transfer through fibrous insulation were also studied.[3,7]

Thermal radiation accounts for 40–50% of the total heat transfer in lightweight fibrous insulation at moderate temperatures.[8] By enhancing the radiative extinction characteristics, the effectiveness of the insulation can be increased tremendously. A method of improving the radiative characteristics is to construct the insulations from hollow fibers or from solid fibers that are coated by thin dielectric layers. Hollow fibers have the advantage of being lighter and of having a lower heat capacity, and hence a faster thermal response, than their solid counterparts. This study examines the radiative characteristics of the individual fibers and those of the packed insulations made of such. Hollow fibers are currently used for lightweight insulation such as in down jackets, sleeping bags, in home insulation, and as thermal insulation in flow systems.[9] Some commercial brands available are the polyester Hollofil and Quallofil manufactured by DuPont.

Previous numerical studies of the hollow fibers have been confined to the scattering from single fibers at normal incidence of radiation, with the fiber material having real refractive indices (nonabsorbing material). Kerker and Matijevic[10] formulated the expressions for the scattering characteristics of concentric infinite cylinders at normal incidence of radiation. Evans et al.[11] performed calculations of the extinction efficiency and the backward component of scattered flux for dielectric hollow fibers subjected to normally incident radiation for a range of fiber sizes and refractive indices. The analytical formulation for the electromagnetic scattering from radially inhomogeneous infinite cylinders at oblique incidence was first presented by Farone and Querfeld,[12] but no numerical computations were made. Samaddar,[13] however, pointed out that their treatment of the conditions along the axis of the cylinder was in error. Indeed, a comparison of their analysis with that of Liou,[14] who presented results for the scattering from solid cylinders at oblique incidence, indicates the omission of a multiplicative factor [i.e., $\exp(-ihz)$ in the

definition[12] of F_n]. This modifies the expressions presented for the scattered fields. However, the other results are not affected and the expressions for the extinction efficiency remain unchanged. This is true for the cylinders whose layers have homogeneous properties, such as homogeneous hollow fibers and coated cylinders. If the layers have radially varying properties, there is no rigorous simple method to solve for the fields, as also noted by Samaddar.[13]

The radiative characteristics of hollow fibers and of solid fibers coated with dielectrics are numerically calculated for different incident directions using Farone and Querfeld's formulation.[12] Averaging over all angles yields the average radiative properties of a single fiber, such as the extinction efficiency, scattering albedo, and backscattered fraction. Based on the independent scattering theory, the single fiber results can be used to compute the extinction coefficient and the radiant conductivity of the insulation. Radiative heat-transfer results representative of room temperature applications of glass and polyester fibrous insulations are presented.

Theory

Single-Fiber Properties

To evaluate the radiative characteristics of packed fiber insulation, it is necessary to compute the extinction and the scattering efficiencies Q_e and Q_s, the single-scattering albedo ω, and the backscatter fraction b for a single fiber. These are based on the solutions of Maxwell's equations along with appropriate boundary conditions. They are a function of the orientation of the fiber relative to the incoming radiation and the angle of observation. For the hollow fibers commonly used, the length of the fiber is of the order of 10^4 μm and the outer diameter is in the range of 20–70 μm. The characteristic wavelength at moderate temperatures (i.e., near room temperature, 300 K) is of the order of 10 μm. The characteristic wavelength at a given temperature is taken to be the wavelength at which the black-body emissive power is a maximum at that temperature, based on Wien's displacement law. The length of the fiber is approximately four orders of magnitude greater than both the diameter of the fiber and the operating characteristic wavelength and can thus be treated as being infinitely long.[15] The end effects can be ignored, and the resulting expressions for the scattering and extinction efficiencies and the scattered radiation intensity for a given incident direction are[12]

$$Q_s=\frac{1}{\alpha}\left[|a_{02}|^2+|b_{01}|^2+2\sum_{n=1}^{\infty}(|a_n|^2+|a_{n2}|^2+|b_{n1}|^2+|b_{n2}|^2)\right] \quad (1)$$

$$Q_e=\frac{1}{\alpha}\mathrm{Re}\left[a_{02}+b_{01}+2\sum_{n=1}^{\infty}(a_{n1}+a_{n2}+b_{n1}+b_{n2})\right] \quad (2)$$

$$I=\frac{1}{\pi\alpha}\left[\left|b_{01}+2\sum_{n=1}^{\infty}b_{n1}\cos(n\zeta)\right|^2+\left|2\sum_{n=1}^{\infty}a_{n1}\sin(n\zeta)\right|^2+\left|a_{02}+2\sum_{n=1}^{\infty}a_{n2}\cos(n\zeta)\right|^2+\left|2\sum_{n=1}^{\infty}b_{n2}\sin(n\zeta)\right|^2\right] \quad (3)$$

where Re indicates the real part. The observation angle ζ is measured in a plane perpendicular to the fiber axis. The zero value of ζ is assigned to the original incident direction. The angle between the incident radiation and the fiber axis is η, as illustrated in Fig. 1. The size parameter α is defined as

$$\alpha=\pi D/\lambda_0 \quad (4)$$

where D is the outer diameter and λ_0 the wavelength of the incident radiation evaluated in the surrounding medium. An assumption of unpolarized incident radiation is implicit in Eqs. (1–3). The scattered radiation propagates along the surface of a cone whose apex angle is $(\pi-2\eta)$. Although not used in the subsequent analysis, Eq. (3) indicates the nature of the scattered radiation. The expressions for the coefficients a_n and b_n are complicated and can be found elsewhere.[12] An error in the expressions for a_n and b_n in Eq. (12) of Farone and Querfeld[12] was noted, where the first term should be $-fJ_n'(fb)$, instead of $-J_n'(fb)$ as presented. The coefficients a_n and b_n depend on the refractive index $\tilde{m}$, which is wavelength dependent. Thus, the radiative properties are spectral quantities.

The fibers are assumed to be randomly oriented in space within the fibrous insulation. For such a random distribution of fiber orientations, the average radiative quantities at each wavelength are obtained by averaging over all incident angles:[6]

$$\bar{Q}_{e,s}=\frac{2}{\pi}\int_0^{\pi/2}Q_{e,s}\,d\eta \quad (5)$$

A bar above the variable is used to indicate its average value. The above method of averaging is consistent with the approximations of the two-flux model used to predict the radiative transfer in fibrous insulation. The backscatter fraction b is defined as the fraction of radiation scattered in the backward facing hemisphere and is given by[3,6]

$$b=\frac{1}{2}-\frac{4}{\pi^2\alpha\bar{Q}_s}\int_0^{\pi/2}G\,d\eta \quad (6)$$

where the expression for G can be obtained from Wang and Tien.[6] Equations (5) and (6) are not valid when the fibers have some preferred orientation or are distributed over the space in some specified directions.

Fibrous Insulation Characteristics

The independent scattering theory is invoked to relate the radiative transfer characteristics of a single fiber to those of the fibrous insulation. Work on packed spheres[16] shows that the particles can be treated as independent scatterers even in dense media as long as the ratio of the interparticle spacing c to the characteristic wavelength λ_0 of the incident radiation evaluated in the surrounding medium is 0.3 or greater. The denseness of packing of the fibers in the insulation can be characterized by f_v, the solid volume fraction. For normal glass fiber insulation, the typical f_v is about 2%.[3] Even if f_v goes up to 50% as in packed/fluidized beds, c/λ_0 is still

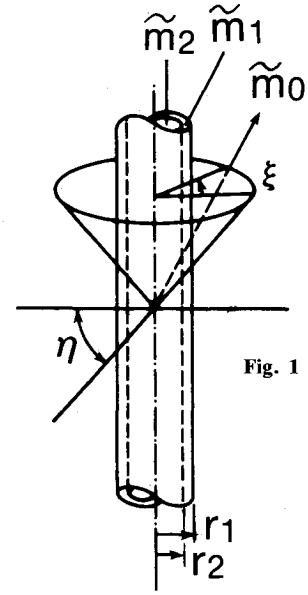

Fig. 1 Coordinate system.

greater than 0.3 and the independent scattering theory holds.[16] The extinction coefficient of a fibrous insulation of volume V containing N randomly oriented fibers of uniform diameter D and length l is[3,6]

$$\sigma_e = lD\bar{Q}_e N/V = 4\bar{Q}_e \hat{f}_v/\pi D \tag{7}$$

where $\hat{f}_v$ is an apparent volume fraction based on the external diameter of the hollow fibers (i.e., the hollow fibers are treated as solid cylinders of the same outside diameter) and is correlated by

$$f_v = \hat{f}_v\left[1-\left(\frac{r_2}{r_1}\right)^2\right],\quad \hat{f}_v = l\frac{\pi D^2}{4}\frac{N}{V} \tag{8}$$

Since the radiative characteristics of the fibrous insulation depend on the wavelength, the total quantities may be obtained by integrating the spectral quantities over all wavelengths with Planck's distribution as the weighting function. The radiant conductivity k_r, based on the two-flux model of radiative transfer, may be defined as

$$k_r = \frac{4\sigma T_m{}^3}{[(1-\omega+2b\omega)\sigma_e]_m} \tag{9}$$

where

$$\frac{1}{[(1-\omega+2b\omega)\sigma_e]_m} = \frac{1}{\sigma T_m^4}\int_0^\infty \frac{e_{b\lambda}(T_m)}{(1-\omega+2b\omega)\sigma_e}\,d\lambda \tag{10}$$

The variation of the optical constants with wavelength has to be considered while evaluating the values of ω, b, and σ_e in the above integral. However, since most of the energy in Planck's distribution is concentrated around the peak wavelength given by Wien's displacement law, a rough estimate of the radiative flux can be made by evaluating the radiative characteristics at this wavelength. This reduces the required computational effort drastically and gives a good leading order estimate. For small wall temperature differences, a radiant conductivity based on the arithmetic mean temperature T_m can be approximated as[6,17]

$$k_r = 4\sigma T_m^3/(1-\omega+2b\omega)\sigma_e \tag{11}$$

where the radiative properties are evaluated at the characteristic wavelength corresponding to T_m, the mean temperature. The optical constants for the fibers are chosen to be those corresponding to this characteristic wavelength. The emissivities of the walls bounding the insulation are neglected in Eqs. (9-11) for heat flux calculations in such optically dense media.

Numerical Scheme

The numerical computation of the radiative characteristics involve calculations of Bessel functions of complex arguments and high orders. Many mathematical operations have to be performed to obtain the values corresponding to each angle of incidence. The numerical error resulting from the numerical roundoff associated with these operations becomes more prominent at large-size parameters and at high values of the refractive index. The numerical error is found to be insignificant for the size parameters α smaller than 10 for moderate values of the refractive index. The computations reported are performed on the DEC VAX 11/750 computer system using double-precision Fortran 77 operating under the Berkeley-UNIX operating software.

The two major contributors to the numerical error are the recursions used to generate Bessel functions and the evaluation of determinants. Bessel functions are generated using the techniques illustrated by Farone and Kerker[18] and Goldstein and Thaler.[19] Backward recursion, which is more numerically stable than the forward recursion for generating Bessel functions, is used. However, for large arguments very high orders of these functions are needed and this leads to a large number of recursive computations. The highest order to start the recursion from is selected as the integer closest to the absolute value of the argument plus a constant. If the absolute value of the argument is greater than 20, the constant is chosen to be the integer closest to half of the absolute value of the argument. Otherwise, the value of the constant is set to 10. If the zeroth-order function resulting from the backward recursion is very large, the value of this constant is decreased. The value of the constant is also decreased if, at any point in the backward recursion, the values of the functions become very large. Here, by large it is meant that the absolute value approaches the largest value possible on the computer. But for practical purposes, it is taken to be 10^{20}. The recursion is started by assigning a zero value to the highest order and an arbitrarily small value close to the smallest positive real number supported by the computer to the next highest. The normalization is obtained by summing over the resulting even orders. The numerical techniques used here are documented in detail elsewhere.[15]

The matrices whose determinants are to be computed become ill-conditioned at high orders. The various elements of the matrix span a large range of orders of magnitude. The matrix is relatively sparse and this precludes the use of maximal pivoting techniques of evaluating the determinants. To overcome this, the columns are swapped so that the diagonal elements are nonzero and are large in magnitude. A direct factorization of the matrix into upper and lower triangular matrices is then performed (LU decomposition) and the determinant is computed by multiplying all the diagonal elements together.

Simpson's rule is used to evaluate the integrals in Eqs. (5) and (6) numerically. The number of intervals used between 0 and $\pi/2$ is 300.

Numerical Results

The cases in this study correspond to moderate temperatures (250–400 K), such as those encountered in building insulation applications and in uses such as in jackets and sleeping bags. The characteristic wavelength range for these temperatures is 7–12 μm. Present manufacturing technology places a lower limit on the diameters of the hollow fibers produced. Commercially, the lower range of diameters available are between 20 and 30 μm. This renders the size parameters between 5 and 10 to be important for these diameters at the temperatures indicated above. Four refractive indices $\tilde{m}_1$, $1.5-i0.5$, $1.5-i0.05$, $3.0-i0.5$, and $3.0-i0.05$, which are representative of the optical constants of glass and polyethylene terepthalate (PET) fibers in the ranges of interest, are selected for the numerical study. The

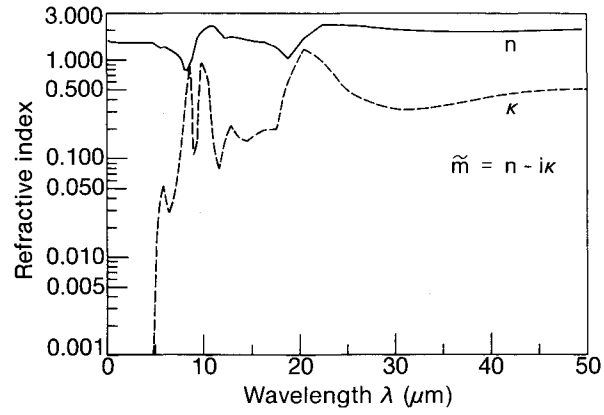

Fig. 2 Complex refractive index for silicate glass.

Table 1 Band-averaged constants of PET

λ,μm	n	κ
4.0–6.8	1.805	0.00327
6.8–9.8	3.648	0.01763
9.8–14.3	2.191	0.01700
14.3–21.0	1.565	0.01114
21.0–100.0	1.955	0.02215

optical constants of glass reported by Hsieh and Su[20] are presented in Fig. 2. The values of these optical constants are irregularly distributed over the spectrum of wavelengths. The composition by percentage of the glass considered is 73.5 SiO_2, 21.3 Na_2O, and 5.2 CaO. Band-averaged constants of PET films[21] are used to approximate the optical constants of polyester fibers, see Table 1. (PET is Mylar manufactured by DuPont.)

Numerical results are presented for solid and hollow fibers whose size parameter range is 0.1–10.0. This corresponds to outside diameters between 1 and 30 μm for wavelengths that are approximately equal to the characteristic wavelength (≈10 μm) at room temperature. The extinction efficiency $\bar{Q}_e$, the scattering albedo ω, and the backscattered fraction factor b for hollow cylinders are presented in Figs. 3–5 for different values of the refractive index $\tilde{m}_1$ and the radius ratio r_2/r_1. Figure 6 presents the values of the extinction coefficient σ_e, and Fig. 7 shows the variation of the radiant conductivity k_r with the diameter D of the fibers.

The results for $r_2/r_1 = 0$ are special cases that correspond to the solid cylinders and are obtained by assigning $\tilde{m}_1 = \tilde{m}_2$ for any non zero r_2/r_1 during the computations. Values computed for a perpendicularly incident electromagnetic wave in the size parameter range of $0.5 < \alpha < 6$ and $\tilde{m}_1 = 1.5$, 2.0, and 2.5 are not reported here, but were obtained to check for consistency with those repoted by Evans et al.[11]

Figures 3a and 3b examine the effect of the complex refractive indices and the hollowness on $\bar{Q}_e$, the averaged extinction efficiency. By increasing either the real or the imaginary (absorptive) part of the complex refractive index $\tilde{m}_1$ while keeping the other part fixed increases $\bar{Q}_e$ on the average over the size parameter range examined. This effect is pronounced at lower sizes ($\alpha < 2$). At large sizes, the values are relatively insensitive to $\tilde{m}_1$ and approach asymptotically to the same value. Making the fibers hollow increases $\bar{Q}_e$ for large sizes and the optimal radius ratio, or the degree of hollowness, depends on the size parameter, see Fig. 4. At small sizes, the value of $\bar{Q}_e$ is reduced by hollowness, but the loss is not significant (Fig. 4). Thus, for small sizes, increasing the refractive index is the most efficient way of increasing the extinction. For the size parameters between 5 and 10, making the fiber hollow will result in higher extinction, the optimum radius ratio being determined from Fig. 4, whereas a change in refractive index is comparatively ineffectual. The values of $\bar{Q}_e$ for solid cylinders agree well with those presented by Wang and Tien.[6]

As κ [Im($\tilde{m}$)] increases, the extinction efficiencies for hollow and solid fibers are less distinguishable if α is large. This is due to the fact that as κ increases, the absorption becomes more significant. At larger α, the wavelength is small compared to the fiber diameter and the fiber wall thickness, except for the thin-walled fibers. The wall thickness, determined by r_2/r_1, is then not a significant parameter in determining the extinction efficiency. The same holds for ω and b.

A similar study of the backscattered fraction b is given in Figs. 3a and 3b. Trends opposite to those reported for $\bar{Q}_e$ are observed. The effect of refractive index is more pronounced at higher-size parameters ($\alpha > 0.5$). By increasing either the imaginary or the real part of the refractive index, the backscatter increases. The backscattering factors for the

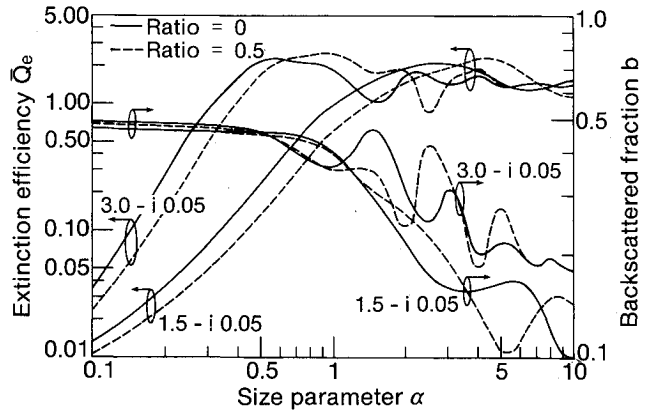

Fig. 3a Extinction efficiency, backscattered fraction (refractive indices 1.5 – *i*0.05 and 3.0 – *i*0.05).

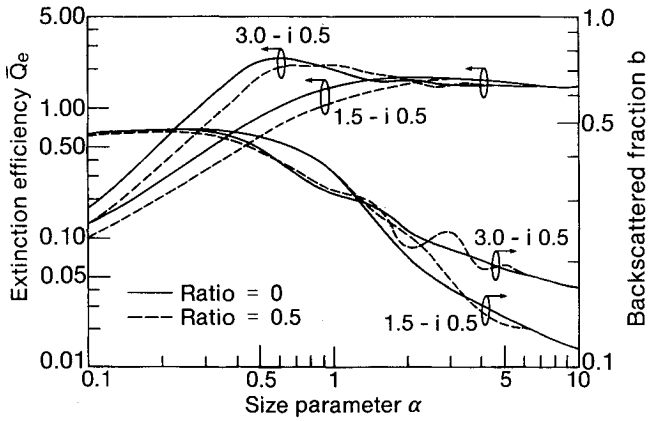

Fig. 3b Extinction efficiency, backscattered fraction (refractive indices 1.5–*i*0.5 and 3.0–*i*0.5).

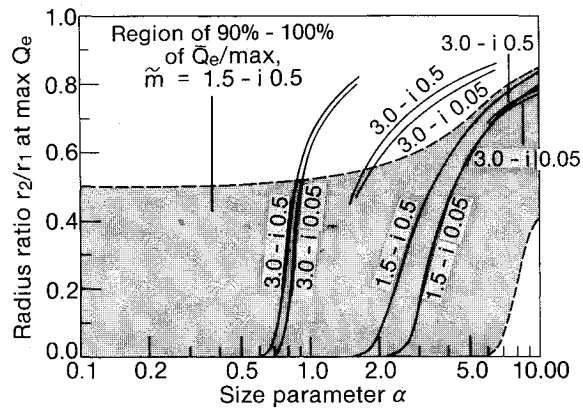

Fig. 4 Optimal radius ratio for maximum extinction efficiency.

hollow and solid fibers are not distinguishable at small-size parameters. As the size parameter α increases, the value of b fluctuates rapidly. However, on the average over the size parameter range being considered, the hollow fibers exhibit higher backscatter than the solid fibers. Fibers with larger absorption index κ show a smoother correlation between the radiative properties and the size parameter than their counterparts with smaller κ values.

The optimal ratio of inner to outside radius, at which the maximum extinction efficiency is obtained, is indicated by Fig. 4. It is a function of the size parameter and the refrac-

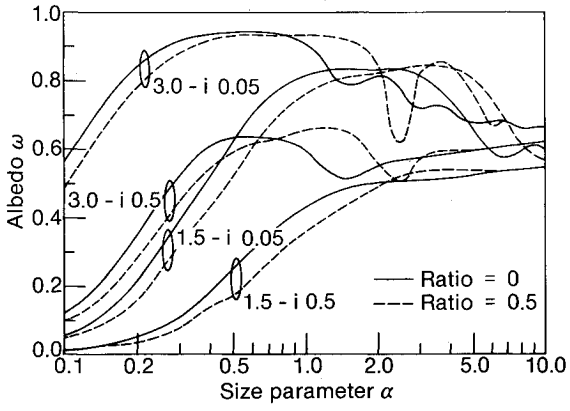

Fig. 5 Single-scattering albedo.

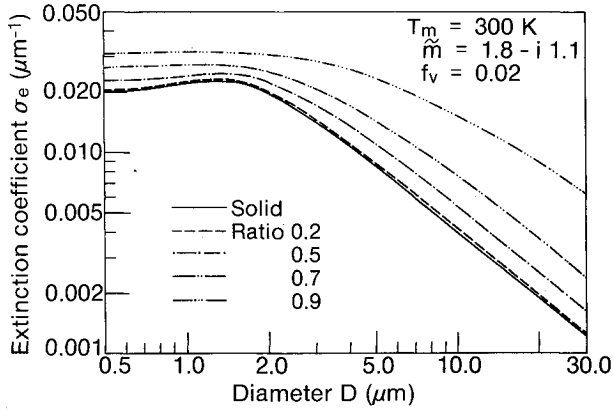

Fig. 6a Extinction coefficient for fixed-volume fraction f_v.

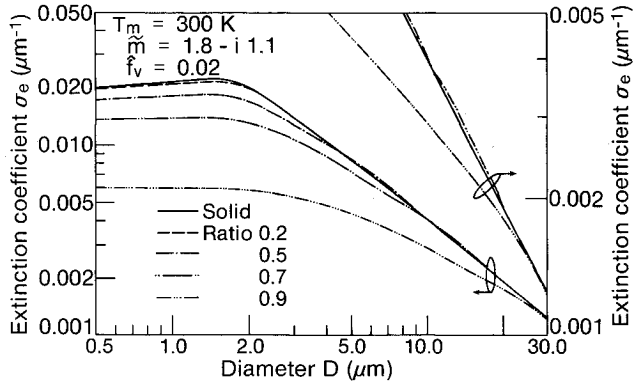

Fig. 6b Extinction coefficient for fixed-number density $\hat{f}_v$.

tive index. For small sizes, the solid cylinder is most efficient with regard to the extinction efficiency. The values of the radius ratio that will give $\bar{Q}_e$ within 10% of the maximum possible value at the same size parameter encompass a broad range. Thus, making a fiber hollow is advantageous at all wavelengths and sizes. For example, it is seen that fibers of refractive index $1.5-i0.5$ can be made hollow to the extent that $r_2/r_1=0.5$ and still have more than 90% of the maximum extinction efficiency that can possibly be achieved at that size parameter. The optimal radius ratio is not a continuous monotonically increasing function of the size parameter. The optimal radius ratio increases until approximately 0.8 as the size parameter increases and then decreases. This is due to the sharp decrease in the absorption component of the total extinction as the walls become very thin. This process is repeated again when the optimal ratio becomes large. However, each such consecutive branch of the optimal curve terminates at slightly higher values of the optimal radius ratio. This is a manifestation of the appreciable absorption of the fibers having larger-size parameters, even when the radius ratio approaches unity. The consecutive branches also become less steep. These phenomena are easily observed in Fig. 4 for $\tilde{m}_1=3.0-i0.5$ and $3.0-i0.05$. The optimal ratios for $\tilde{m}_1=1.5-i0.5$ and $1.5-i0.05$ will show similar behavior if extended past size parameter 10. Increasing the imaginary part of the refractive index increases the absorption, which leads to a more hollow optimal fiber configuration.

Figure 5 shows the change of the single-scattering albedo ω decreases with increasing the imaginary part of the radiative index.

Figures 3–5 indicate that the best combination in the range of practical interest is to have a small refractive index to ensure high backscatter and an increased hollowness to enhance both the backscatter and the extinction. The plot of the extinction coefficient σ_e at room temperature for hollow fiber insulation vs the outside diameter D (Fig. 6) indicates that hollowness is desirable. The value of $\tilde{m}_1$ in Figs. 6 and 7 is chosen to be $1.8-i1.1$ from Fig. 2, since it corresponds to that of glass at the characteristic wavelength at room temperature. Two types of cases are considered: fixed weight per unit volume f_v and fixed $\hat{f}_v$, which is indicative of a constant volumetric number density.

If f_v is kept constant, the effect of increasing the hollowness is very significant, as can be seen from Fig. 6a. Keeping f_v and the outside diameter D fixed and increasing the hollowness of the fibers increases the number density N/V of the fibers in the insulation, as is indicated by Eq. (8). The corresponding increase in the extinction coefficient is directly proportional to this jump in the number density [Eq. (7)], making an increase in the hollowness very advantageous when the total weight is to be kept fixed. The high extinction coefficient obtained by constructing insulation of small-diameter solid fibers can now also be achieved by using hollow fibers of larger diameters. This presents an alternate method of obtaining high extinction values.

Figure 6b indicates that for constant $\hat{f}_v$ hollowness has a small effect on the extinction coefficient of the insulation composed of fibers whose outside diameters are between 10 and 30 μm. An increase in the radius ratio keeps the value of the extinction coefficient fairly constant, but reduces the weight of the insulation tremendously. The optimal hollowness for the maximum extinction efficiency of the insulation depends on the outside diameter of the fiber for a given operating condition. Since the peak extinction at a given T_m occurs for the insulation made of solid fibers with outside diameters between 1 and 5 μm, such a solid-fiber insulation would constitute the most effective radiation extinguisher. If fibers with diameters in the range of 10–30 μm are used, it is advantageous from the viewpoint of extinction to make them hollow. However, the corresponding extinction coefficient of such insulation is less than the peak exhibited by the insulation composed of solid fibers with diameters between 1 and 5 μm. The insulation made of hollow fibers in the diameter range 10–30μm is lighter and has a smaller thermal capacity than the insulation of solid fibers in the diameter range of 1–5 μm with the same $\hat{f}_v$. The gain in the extinction coefficient by using solid fibers in the diameter range of 1–5 μm is offset by the higher weight of the insulation. Similarly, the lower value of the extinction coefficient offered by hollow fibers with larger outside diameter is balanced by the lower weight and the smaller thermal capacity of the insulation.

When f_v is kept constant, hollowness will improve the extinction characteristics slightly and greatly reduce the weight. But when the total weight f_v is maintained constant and the hollowness is increased, the extinction coefficient increases very significantly. Similar trends are observed when the four

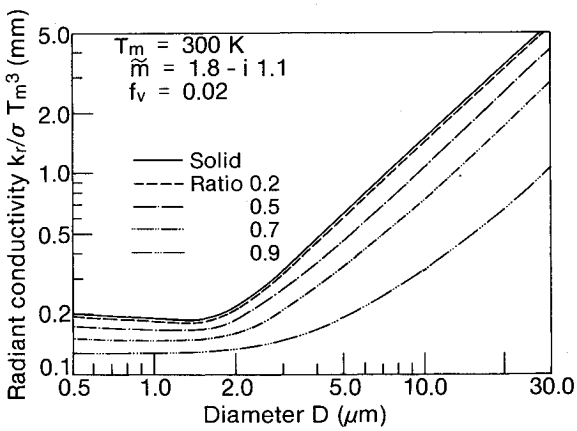

Fig. 7a Radiant conductivity for fixed-volume fraction f_v.

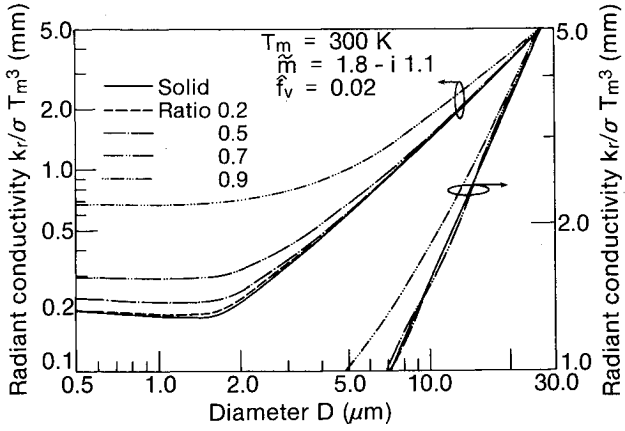

Fig. 7b Radiant conductivity for fixed-number density $\hat{f}_v$.

different refractive indices considered previously are used. The peak extinction occurs at lower diameters if T_m is increased and $\tilde{m}_1$ remains the same. Increasing either the real or imaginary part of the $\tilde{m}_1$ shifts the peak of the extinction coefficient curve to lower diameters and increases the value of the peak.

The variation of the radiant conductivity k_r of the insulation vs the outside diameter D at room temperature $T_m = 300$ K is depicted in Figs. 7a and 7b. Equation (7) has been used to compute the values presented in Fig. 7. If the weight f_v of the insulation is kept constant, lower radiant conductivities are obtained by using hollow fibers. If $\hat{f}_v$ is kept constant, the lowest values of k_r are exhibited by the solid-fiber insulations and the diameter of the fibers corresponding to this minima is in the range of 1-5 μm. An increased hollowness in fibers with diameters of 10-30 μm decreases the radiant conductivity of the insulation and thus lowers the radiative heat loss. Again, the optimal radius ratio depends on the outside diameter of the fibers for fixed operating conditions and fixed $\hat{f}_v$. An average in either the real or imaginary part of the complex refractive index decreases k_r on the average. The value of the diameter at which the absolute minimum occurs at a given radius ratio and refractive index induces with increasing T_m, the mean temperature.

Solid fibers of the same optical constants as those considered above and coated with thin dielectric coatings are also studied. For a ratio of the outer radius to the inner radius of 1.01, the extinction efficiency and the backscattered fraction are slightly increased only if the dielectric coating has a high refractive index ($\tilde{m}_1 > 4.0$). Coatings with a small index have a detrimental effect. For a radius ratio of 1.1, a slight gain in the extinction is obtained for coatings of moderate refractive index ($1.1 < \tilde{m}_1 < 4.0$). Table 2 presents some values of $\bar{Q}_e$ for a size parameter based on the inside diameter of 5. The optimal refractive index of the dielectric coating for a given size and radius ratio can be determined; however, it is not worthwhile because of the reasons stated above.

Table 2 $\bar{Q}_e$ for cylinders coated with dielectrics ($2\pi_2/\lambda = 5.0$)

$\tilde{m}_2$	No coating	$\tilde{m}_1 = 1.1$	$\tilde{m}_1 = 1.5$	$\tilde{m}_1 = 2.0$	$\tilde{m}_1 = 3.0$
		$r_1/r_2 = 1.01$			
1.5 − i0.05	1.532	1.517	1.512	1.496	1.496
1.5 − i0.50	1.501	1.489	1.496	1.499	1.473
3.0 − i0.05	1.411	1.402	1.416	1.430	1.463
3.0 − i0.50	1.495	1.484	1.493	1.498	1.472
		$r_1/r_2 = 1.10$			
1.5 − i0.05	1.532	1.396	1.376	1.313	1.432
1.5 − i0.50	1.501	1.390	1.466	1.554	1.462
3.0 − i0.05	1.411	1.324	1.481	1.575	1.673
3.0 − i0.50	1.495	1.397	1.488	1.515	1.514

Conclusions

In the size parameter range of 5-10, hollow fibers exhibit higher backscatter and higher extinction efficiencies than exhibited by solid fibers. Higher values of the complex refractive index promote higher backscatter in this range, but have a very small effect on the extinction. At moderate temperatures, the insulation made of hollow fibers with outside diameters of 10-30 μm is more efficient than one made of solid fibers of the same outside diameter when $\hat{f}_v$ is kept constant. In this case, the insulation of hollow fibers exhibits a higher extinction coefficient and lower radiant conductivity and offers lower weight and smaller thermal capacity. If the solid volume fraction f_v is kept fixed, hollow fibers enhance the extinction characteristics of insulation very significantly. Coating solid fibers with thin layers of dielectric offers no appreciable enhancement of the radiative properties of the fibrous insulation unless the coating is thick or has a high dielectric refractive index.

A detailed study of the radiative transfer characteristics of the insulation by integrating the spectral quantities over all wavelengths, such as indicated by Eq. (10), and at different temperatures would require tremendous amounts of computer time. As pointed out earlier, the numerical computations are prone to errors and care must be taken to avoid the propagation of these numerical errors. To obtain accurate values for practical applications, within reasonable computation times, the calculations should be carried on large, fast, computers that carry many significant digits.

References

[1]Bankvall, C.G., "Heat Transfer in Fibrous Materials," *Journal of Testing and Evaluation,* Vol. 1, 1973, pp. 235-243.

[2]Kinoshita, I., Kamiuto, K., and Hasegawa, S., "Study of Simultaneous Conductive and Radiative Heat Transfer in High Porosity Materials," *Proceedings of the 7th International Heat Transfer Conference,* Vol. 2, 1982, Hemisphere Publishers, New York, pp. 505-510.

[3]Tong, T.W. and Tien, C.L., "Radiative Heat Transfer in Fibrous Insulations—Part I: Analytical Study," *Journal of Heat Transfer,* Vol. 105, 1983, pp. 70-75.

[4]Houston, R.L. and Korpela, S.A., "Heat Transfer through Fiberglass Insulation," *Proceedings of the 7th International Heat Transfer Conference,* Hemisphere Publishers, New York, Vol. 2, 1982, pp. 499-504.

[5]Chan, C.K. and Tien, C.L., "Radiative Transfer in Packed Spheres," *Journal of Heat Transfer,* Vol. 96, 1974, pp. 52-58.

[6]Wang, K.Y. and Tien, C.L., "Radiative Heat Transfer through Opacified Fibers and Powders," *Journal of Quantitative Spectroscopy & Radiative Transfer,* Vol. 30, 1983, pp. 213-223.

[7]Tong, T.W. and Tien, C.L., "Analytical Models for Thermal Radiation in Fibrous Insulations," *Journal of Thermal Insulation,* Vol. 4, 1980, pp. 27-44.

[7]Tong, T.W. and Tien, C.L., "Analytical Models for Thermal Radiation in Fibrous Insulations," *Journal of Thermal Insulation,* Vol. 4, 1980, pp. 27-44.

[8]Tong, T.W., Yang, Q.S., and Tien, C.L., "Radiative Heat Transfer in Fibrous Insulations—Part II: Experimental Study," *Journal of Heat Transfer,* Vol. 105, 1983, pp. 76-81.

[9]Wang, K.Y. and Tien, C.L., "Thermal Insulation in Flow Systems: Combined Radiation and Convection through a Porous Segment," *Journal of Heat Transfer,* Vol. 106, 1984, pp. 453-459.

[10]Kerker, M. and Matijevic, E., "Scattering of Electromagnetic Waves from Concentric Cylinders," *Journal of the Optical Society of America,* Vol. 51, 1961, pp. 506-508.

[11]Evans, L.B., Chen, J.C., and Churchill, S.W., "Scattering of Electromagnetic Radiation by Infinitely Long, Hollow, and Coated Cylinders," *Journal of the Optical Society of America,* Vol. 54, 1964, pp. 1004-1007.

[12]Farone, W.A. and Querfeld, C.W., "Electromagnetic Scattering from Radially Inhomogenous Infinite Cylinders at Oblique Incidence," *Journal of the Optical Society of America,* Vol. 56, 1966, pp. 476-480.

[13]Samaddar, S.N., "Scattering of Plane Electromagnetic Waves by Radially Inhomogeneous Infinite Cylinders," *Nuovo Cimento,* Vol. 66B, 1970, pp. 33-51.

[14]Liou, K.-N., "Electromagnetic Scattering by Arbitrarily Oriented Ice Cylinders," *Applied Optics,* Vol. 11, 1972, pp. 667-674.

[15]Wang, K.Y., "Thermal Insulation in Flow Systems," Ph.D. Dissertation, University of California, Berkeley, 1983.

[16]Brewster, M.Q. and Tien, C.L., "Radiative Transfer in Packed/Fluidized Beds: Dependent vs. Independent Scattering," *Journal of Heat Transfer,* Vol. 104, 1982, pp. 573-579.

[17]Tong, T.W., "Thermal Radiation in Fibrous Insulations," Ph.D. Dissertation, University of California, Berkeley, 1980.

[18]Farone, W.A. and Kerker, M., "Light Scattering from Long Submicron Glass Cylinders at Normal Incidence," *Journal of the Optical Society of America,* Vol. 56, 1966, pp. 481-487.

[19]Goldstein, M. and Thaler, R.M., "Recurrence Techniques for Calculation of Bessel Functions," *Mathematical Tables and Other Aids of Computation,* Vol. 13, 1959, pp. 102-108.

[20]Hsieh, C.K. and Su, K.C., "Thermal Radiative Properties of Glass for 0.32 to 206 microns," *Solar Energy,* Vol. 22, 1979, pp. 37-43.

[21]Tien, C.L., Chan, C.K., and Cunningham, G.R., "Infrared Radiation of Thin Plastic Films," *Journal of Heat Transfer,* Vol. 94, 1972, pp. 41-45.